European Geothermal Congress 2019

Den Haag, The Netherlands, 11-14 June 2019

# Contribution of SWIR to the Clay Signature of Permeable Fracture Zones in the Granitic Basement. Overview of Soultz and Rittershoffen wells.

Carole Glaas[1,2,3], Jeanne Vidal[4], Patricia Patrier[3], Daniel Beaufort[3], Albert Genter[2]

[1]University of Strasbourg, CNRS, UMR 7516 IPGS, 5 Rue René Descartes, 67084 Strasbourg Cedex, France

[2]ES-Géothermie, Bat Le Belem 5 rue de Lisbonne, 67300 Schiltigheim, France

[3] University of Poitiers, CNRS UMR 7285 IC2MP, HydrASA, Bat B8 rue Albert Turpain, TSA51106, F-86073 Poitiers Cedex 9, France

[4] University of Chile, FCFM, Dept. of Geology, Andean Geothermal Center of Excellence (CEGA), Plaza Ercilla 803, Santiago, Chile

carole.glaas@es.fr

**Keywords:** geothermal, fractured granite, cuttings, short wave infrared (SWIR) spectroscopy, hydrothermal alteration, illite

## ABSTRACT

The high potential of the Upper Rhine Graben (URG) for geothermal relies on more than 30 years of expertise in crystalline geothermal reservoirs developed in Soultz (France), the near presence of direct users in the area of the Eurometropolis of Strasbourg and undeniably, the acceptance of the population and the presence of investors. Hence, Strasbourg area is very attractive and is very active in the development of deep geothermal plants. In this context, this study proposes an innovative method of geothermal exploration to detect the highly hydrothermally altered zones corresponding to permeable fracture zones (FZ). They are acting as natural pathways for the fluid in the crystalline rocks of the URG. Applied on cuttings of granite samples with reduced costs and time, the short wave infrared (SWIR) spectroscopy method was realized on geothermal wells from Northern Alsace (Soultz, Rittershoffen) for calibration. Indeed, the FZ of these wells were first characterized by structural and mineralogical studies done from borehole image logs and cuttings analysis respectively. In the Rittershoffen wells, the occurrence of small crystallites of illite and illite-smectite mixed layers minerals (<10% smectite) were systematically and spatially linked with the occurrence of permeable FZ and thus provide specific clay signatures. In the Soultz wells, mineralogy and FZ structure were deeply studied with core samples descriptions. SWIR spectra were acquired on more than 2400 cuttings in Soultz and Rittershoffen wells. The area of the SWIR peak at 2200 nm wavelength correlates with the amount of illitic minerals and can thus be a direct indicator of argilization and alteration. Observations show that SWIR results correlate with the former X-ray diffraction (XRD) results, binocular magnifier or core observations identifying the several granitic facies affected by hydrothermal alteration. Higher the hydrothermal alteration is and higher the SWIR signal is. SWIR spectroscopy is thus a promising tool to estimate the alteration intensity, and could be a complementary tool for the characterization of FZ architecture. Using routinely field SWIR spectroscopy on crystalline cuttings could be a pioneer method to characterize FZ and their permeability at early stages of geothermal exploration wells.

## 1. INTRODUCTION

The development of the SWIR method as a tool for clay quantification makes sense in the context of developing the deep geothermal expertise in fractured granitic reservoirs. Hence, a better understanding of highly argilized zones corresponding to permeable fracture zones which are acting as natural pathways for the fluid in the crystalline rocks of the URG and their contribution to the well productivity or injectivity is a key point for geothermal achievement (Dezayes et al., 2010; Ledésert et al., 2010, 1993; Rotstein et al., 2006; Sausse et al., 2010; Sausse and Genter, 2005; Vidal and Genter, 2018). Indeed, a better understanding of permeable zones localization will bring a precise knowledge of the several FZ that the well encounters. This will help to design optimized well implementations for new projects but will also help to precisely plan further chemical stimulations in case of well with reduced injectivity or productivity index. Beyond these objectives, the SWIR method is also rapid in terms of acquisition time and presents reduced costs. Because of mineralogy similarities, the applicability of the method could extend to other geothermal projects under development in the Strasbourg area, projects which both target the granitic

fractured basement of the URG as geothermal reservoir.

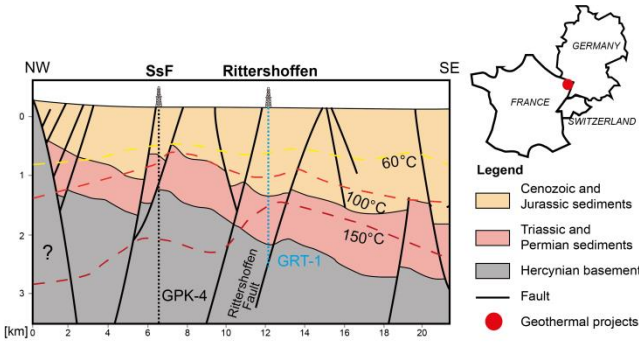


**Figure 1: NW-SE Geological cross section through the Soultz GPK-4 well and the Rittershoffen GRT-1 well.**

## 2. GEOLOGICAL SETTING

### 2.1. Soultz and Rittershoffen sites

In France in 2019, 2 deep geothermal plants exploiting a deep fractured granite are operating (Rittershoffen, Soultz), producing a total of 24 MWth for industrial uses and 1.7 MWe for the electrical grid. Both projects target the granitic basement as geothermal reservoir. The Soultz researches started with the Hot Dry Rock (HDR) concept which deals with the creation of an artificial heat exchanger into massive granitic rocks (Garnish, 1985; Gérard et al., 1984; Gérard and Kappelmeyer, 1987; Kappelmeyer, 1991). By drilling, natural brines were encountered into fractured and altered zones bearing hydrothermal minerals (Genter et al., 2010). Thus the project slowly evolved from the pure HDR concept to the Enhanced Geothermal System (EGS) concept. That could be characterized as a poorly connected hydrothermal system. The Soultz site is now composed of 5 deep wells which in fact revealed numerous permeable FZ (Genter et al., 2010). The GPK-4 well which will be detailed here was drilled vertically from 0 to about 2100 m and was deviated to the south to 5260 m depth (Dezayes et al., 2005). It crosses the tertiary and secondary covers before reaching the top of the granitic basement at 1418 m depth. Six main permeable FZ associated were found in the granitic section (Dezayes et al., 2010). Then, the Rittershoffen project was initiated in 2008 as an EGS project, and the target was to develop the reservoir through the Rittershoffen normal fault by drilling two deep wells GRT-1 and GRT-2. The production well GRT-2 revealed a high productivity index without any stimulation embracing a hydrothermal concept (Figure 1) (Baujard et al., 2017). Achieved in 2016, this project turned out to be a great success. The GRT-1 injection well which will be detailed here was drilled near-vertical, crossing the sedimentary cover from 0 to 2213 m measured depth (MD) where it reached the granitic basement down to 2580 m MD. Two main permeable FZ are intersected at 2326 and at 2368 m MD (Glaas et al., 2018; Vidal et al., 2017). Observations conducted on the cores of the EPS-1 well from Soultz evidence a multiscale fracture network (Genter and Traineau, 1996).Small scale fractures with no evidence of displacement are filled by carbonates, chlorite, iron oxides, epidote and sulphides; and faults visible at core scale are filled by geodic quartz, carbonates, barite and clay minerals. In the case of the Rittershoffen wells, the largest faults are observed because only cutting samples and acoustic image logs are available and thus, small fractures are hardly observed. The term FZ will be generally used in this study for closely spaced fractures of cm-thick observed at borehole scale.

### 1.1. Granitic basement

The Cenozoic rift of the URG(Villemin and Bergerat, 1987) is composed of several types of Paleozoic granites covered by secondary and tertiary sediments. In the Soultz wells, a porphyritic granite composed of potassic feldspar megacrystals (MFK) as well as biotite, plagioclase, and primary quartz is observed as well as a two-mica granite composed of biotite and muscovite, the most frequently in the deepest part of the wells (Dezayes et al., 2005; Genter, 1989; Genter et al., 1999; Traineau et al., 1992). This fractured granitic basement is the seat of fluid circulations through big convection cells where FZ are the main pathways for fluids. In response to these fluid circulations, the granitic rocks experienced hydrothermal alteration. Several grades of hydrothermal alteration are distinguished, and were observed on core samples and cutting samples (Genter, 1989; Genter and Traineau, 1996; Glaas et al., 2018; Traineau et al., 1992)(Figure 3). Mineralogy was also deeply studied with XRD analyses (Dezayes et al., 2005; Hooijkaas et al., 2006; Ledésert et al., 1999, 2009; Meller and Ledésert, 2017; Vidal et al., 2018b) (Figure 2). Based on Soultz observations, a low grade alteration is characterized by chlorite (HLOW), a moderate grade is characterized by minor chlorite, illite and the total alteration of biotite (HMOD), the high grade is characterized by higher amounts of illite (HHIG). The extreme alteration grade is characterized by only high amounts of illite and secondary quartz (in the cuttings) which fill veins close to the fracture cores (HEXT). Finally, the VEIN facies is related to the highest amount of secondary quartz due to the presence of a fracture core filled by secondary hydrothermal quartz.

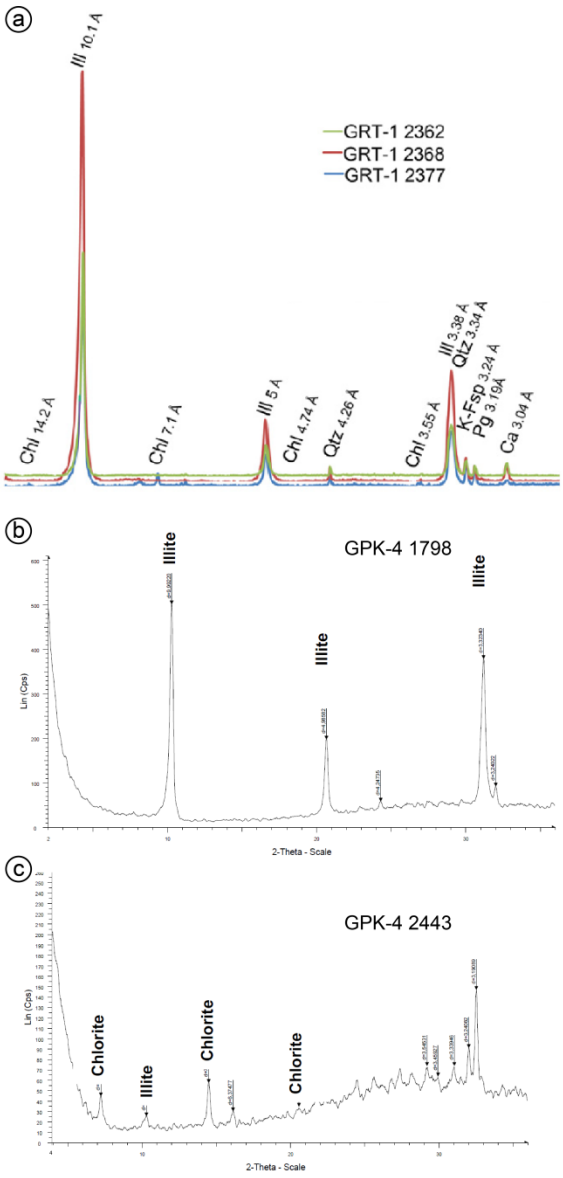


**Figure 2: XRD diffraction patterns a. of the clay fraction in the GRT-1 well main FZ, after Vidal et al., (2018). b. of a vein alteration facies in the GPK-4 well (untreated sample), after (Dezayes et al., 2005). c. of a vein alteration facies in GPK-4 (untreated sample). The chlorite peaks are still visible despite the occurrence of illite, indicating percentage of mixing rock, after Dezayes et al., (2005).**

## 2. MATERIALS AND METHODS

### 2.1. Materials

The cuttings (chip samples) collected during the drilling of the wells are first washed and then dried on-site, by the mud logger unit. In the case of the GRT-1 well and the GPK-4 well from 4727 to 5260 m, the cuttings were sampled every 3-meters in depth in these 8’’1/2 sections. Thus, one bag of cutting represents roughly 100L of rock. For the GPK-4 well in the 12’’1/4 section from 1400 to 4727 m, one bag of cutting represents roughly 200L of rock. For this study, 122 cuttings were analysed in the GRT-1 well and 610 cuttings were analysed in the GPK-4 well. The sampling presented in this study encompasses all the facies presented in the section before. The average size of the cuttings grains varies between 0.5 and 2 mm in each sample. This cutting size can be highly influenced by other parameters like the drilling tool wear. For this reason and as the cutting size influences the SWIR intensity (higher the grain size is, higher the SWIR intensity is), the changes of drilling tool are also presented in this work (Figure 5 andFigure 7). In the GPK-4 well, the cutting samples can present low reliability from 1400 to 4700 m because of a high amount of biotite surely due to mixing of the cuttings during their ascent in the well (Dezayes et al., 2005). The occurrence of such bias is represented by an interpretative facies” (INT) (Figure 7).

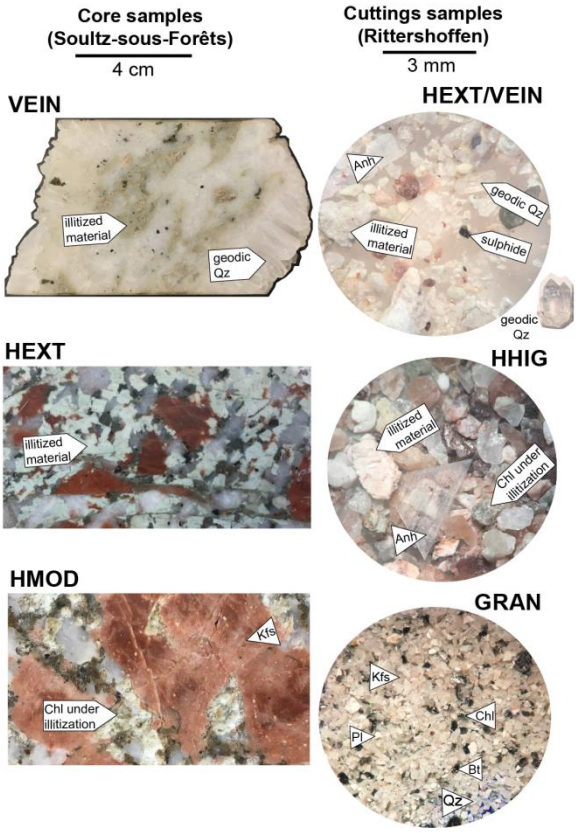


**Figure 3: Mineralogy and its corresponding alteration facies. Observed from cores (left, Soultz-sous-Forêts) and from cuttings (right, Rittershoffen).**

### 2.2. Acquisition method

In total, 732 samples were analyzed from GRT-1 well and 239 from GPK-4 well with ASD TerraSpec 4 Standard Res Mineral Analyzer (Panalytical) equipped with two SWIR detectors. The domain of acquisition is 350 nm- 2500 nm with a spectral resolution of 3 nm at 700 nm and 10 nm from 1400 to 2100 nm. The scanning time of 100 milliseconds allows carrying out rapidly the acquisition for the whole the granitic sections. The wavelength reproducibility is 0.1 nm

with an accuracy of 0.5 nm. Before acquisition the ASD TerraSpec needs a warming-time around 30 minutes. A calibration with a reference material "Spectralon" provided with the machine needs to be conducted also before the first acquisition but also regularly during the acquisition (every 2 hours) (Hébert, 2018). After acquisition, SWIR spectra were processed with the Spectral Swagger (TSS), an in-house Visual Basic macro that runs on Microsoft Excel (Hébert, 2018). First, the baseline was removed automatically by the software and then, spectra were fitted with few Gaussian curves. To create a profile simulation, the user has to fix the position and the half width at half maximum (HWHM). The height parameter is automatically deduced from the baseline-removed spectra, its initial height equals 90% of the Y-axis value of the baseline-removed spectra at the Gaussian centre wavelength. The user can configure which parameter will be allowed to change. Finally, the simulated profile is the sum of all Gaussian curves. The quality of the fit between simulated and observed profile is also verified with the weighted profile R-factor (Rwp) commonly used in Rietveld refinements (Toby, 2006). For this study, six Gaussian curves were used to fit the spectra from 1820 to 2300 nm (Figure 4a). For the GRT-1 well, position and HWHM were locked for each simulation profile. However, different sets of position and HWHM were used. The simulation profiles were accepted with a Rwp lower than 0.05. For the GPK-4 well, with regard to the high amount of profiles calculated, position and HWMH were free for each simulation profile. Four Gaussian curves were used to fit the absorption band from 1900 to 2060 nm (Figure 4a). Because this absorption band is related to water, its variation is influenced by the environmental conditions of acquisition (room humidity). Two Gaussian curves were used to fit the absorption band from 2200 to 2255 nm. These absorption bands are associated with mineralogical feature.

### 2.3. Mineralogical identification

The main curve, located between 2206 and 2214 nm and called the "2200wvl" is associated with 'AlOH' feature representing Al-rich dioctahedral clays (Pontual et al., 1997). The smaller curve that creates a shoulder, located between 2247 and 2253 nm and called "2250wvl" is more complex in terms of feature. Gaussian curves used to fit the spectra from 2300 to 2400 nm are not presented in this study because it is focused on relative quantification of illitic minerals associated with the 'AlOH' feature. This methodology is only used for a relative quantification of clay minerals. From the comparison with literature spectra (Figure 4b), it appears that illite presents a sharp peak at 2200 nm. The influence of chlorite in the 2200 peak is low, but the influence of biotite and muscovite in this 2200 peak is considerable (Figure 4b). As the mineralogy of these wells where thoroughly described we can assume that the 2200 nm peak represents illite variations excepted in the GRT-1 well from 2420 to 2515 m where highest amounts of biotite were observed (Figure 5) and in the GPK-4 well where high concentrations of biotite were observed in the cuttings from 4400 to 4796 m and where the GR2M was observed from to 4814 to 4262 m (Figure 7).

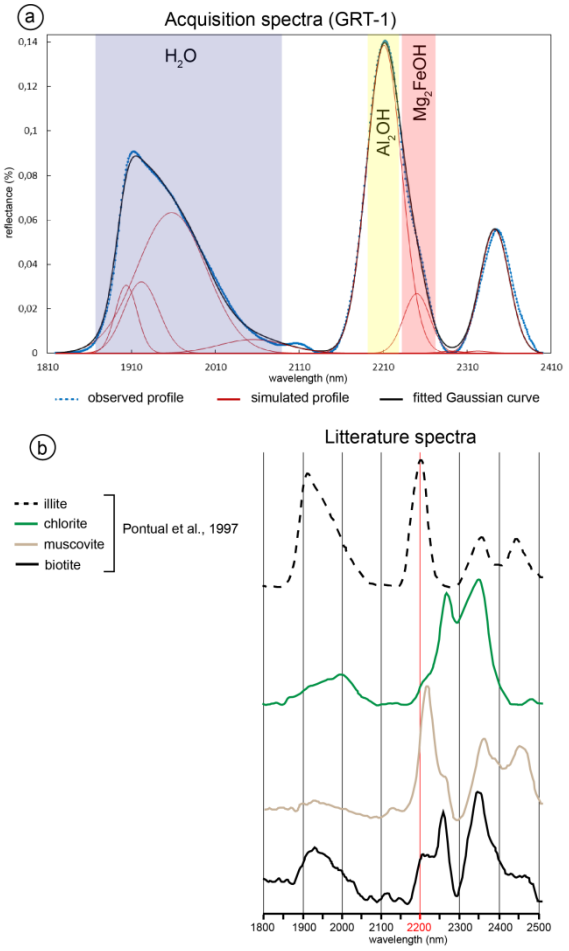


**Figure 4: a. Example of an absorption spectra and the simulated profile in the GRT-1 well at 2420 m. b. Reference spectra from literature of illite, chlorite and biotite.**

### 2.4. Intra-sample variability

As each cutting represents sections of drilled rocks (see section 2.1.) and as the cuttings could not be homogeneously mixed in the bag, several measurements were regularly carried out on the same cutting bag. In the GRT-1 well 10 measurements were done on the same cutting bag while in the GPK-4 well only 5 measurements were done on the same cutting bag as lowest cutting quantities were available. With these several measurements on the same samples, error bars were then calculated in order to observe the range of variation of the data (Figure 5 andFigure 7).

## 3. RESULTS

### 3.1. GRT-1 well

In the granitic part of GRT-1, five zones were distinguished on the basis of SWIR features (Figure 5).

The deepest section, from 2580 to 2510 m MD (2563 to 2493 m true vertical depth (TVD)), is characterized by constant values; the total area is around 20 a.u. (arbitrary unit – area of the Gaussian curve), and the 2200wvl around 5 a.u. (Figure 5). A local increase is observed for the sample at 2536 m MD (2519 m TVD) for the 2200wvl and the total area. This section corresponds petrographicaly to the unaltered granite (GRAN_OX). The origin of the heterogeneity at 2536 m MD still has to be determined.

The second section, from 2510 to 2380 m MD (2493 to 2365 m TVD), is characterized by constant values except from 2470 to 2434 m MD where the curves present small variations (Figure 5). The total area is between 17 and 29 a.u. and the 2200wvl between 5 and 10 a.u. This section corresponds to the low to moderately altered granite (HLOW, HMOD) with a low density of natural fractures. The origin of the heterogeneity at 2420 m MD still has to be determined.

The third section, from 2380 to 2330 m MD (2365 to 2315 m TVD), is characterized by scattered values; the total area is between 22 and 40 a.u., and the 2200wvl between 7 and 13 a.u.. This section corresponds to the main permeable FZ. Within this section, from 2354 to 2371 m MD, the total area presents the lowest values, between 21 and 31 a.u. The lowest values for the water feature (9 to 14 a.u.) are observed for samples from 2365 to 2368 m MD. This subsection corresponds to the core of the FZ composed of opened fractures filled by secondary quartz (VEIN). The local decrease for the sample at 2388 m MD (20 a.u. for the total area and 9.5 a.u. for the water feature) correlates an opened fracture observed in the acoustic image logs (Figure 6c). Above the core of the FZ, higher values of total area, between 28 to 40 a.u. fit the high values of the water feature (15 to 20 a.u.), corresponding to the damage section of the FZ (HEXT). This section corresponds also to a considerable temperature anomaly (Figure 5).

The fourth section, from 2330 to 2255 m MD (2315 to 2241 m TVD), is characterized by quite stable values of the 2200wvl except for samples from 2290 to 2280 m MD. This section corresponds to highly altered granite with a cluster of opened fractures observed in acoustic images from 2290 to 2280 m MD.

The fifth section, from 2255 to 2220 m MD (2241 to 2207 m TVD), is characterized by stable values; around 13 a.u. for the total area, 5 a.u. for the 2200wvl and 1 a.u. for the 2250wvl. It corresponds to the reddish granite (RED) (Figure 5).

As a summary, the intra-sample variability of the 2200wvl shows the highest values for the samples at 2536 m, 2418 m and 2358 m, whereas the variability of the water feature shows the highest values for the samples located at 2358 m and at 2350 m, in the main FZ.

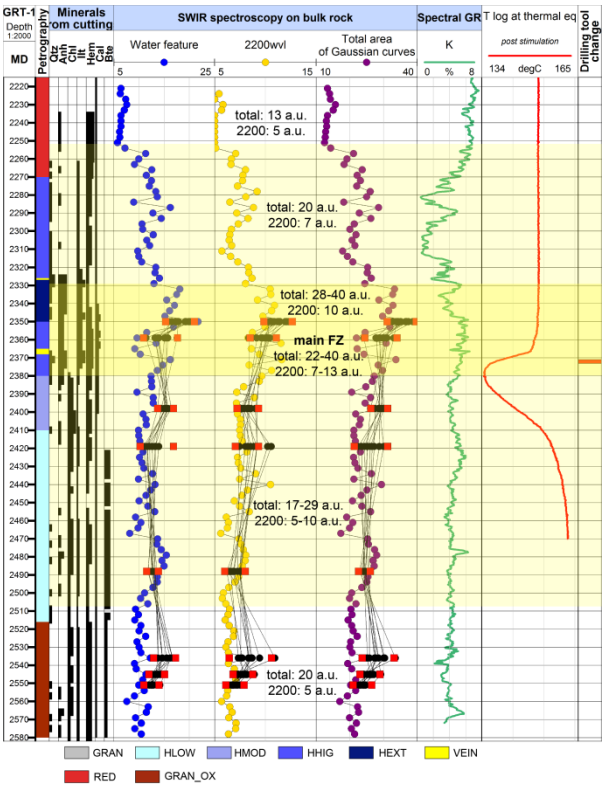


**Figure 5: Composite log of the GRT-1 well presenting the petrography observed on cuttings with the associated minerals quantity, the SWIR results with the water feature, 2200wvl and the total area, the potassium (K) from the spectral gamma ray (GR), the temperature log acquired at temperature equilibrium and the drilling tool change.**

The main FZ of the GRT-1 well from 2350 to 2370 m is composed of several partly opened fractures which are contributing to the well productivity by bearing 70% of the flow (Baujard et al., 2017; Vidal et al., 2017). With the SWIR signal of illite (2200wvl) we can clearly distinguish the main FZ from 2350 to 2370 m which is characterized by scattered values of the 2200wvl from 7 to 13 a.u. (Figure 6). This main FZ surrounds a quartz vein observed on cuttings which is associated to an open permeable FZ observed on the acoustic image logs (Figure 6c). The highest alteration grade (HEXT) is observed above this section, from 2326 to 2350 m and thus is associated with the highest surface area of the 2200wvl (Figure 6). We can also clearly distinguish 3 localized fractures at 2328 m (Figure 6 and 6a), at 2359 m

(Figure 6 and 6b) and at 2368 m (Figure 6 and 6c). These 3 partly opened fractures are characterized by lowest values of the 2200wvl associated with depleted zones in K and with open factures visible on the acoustic image logs (Figure 6). They are associated with a large negative temperature anomaly and mud losses during drilling operations.

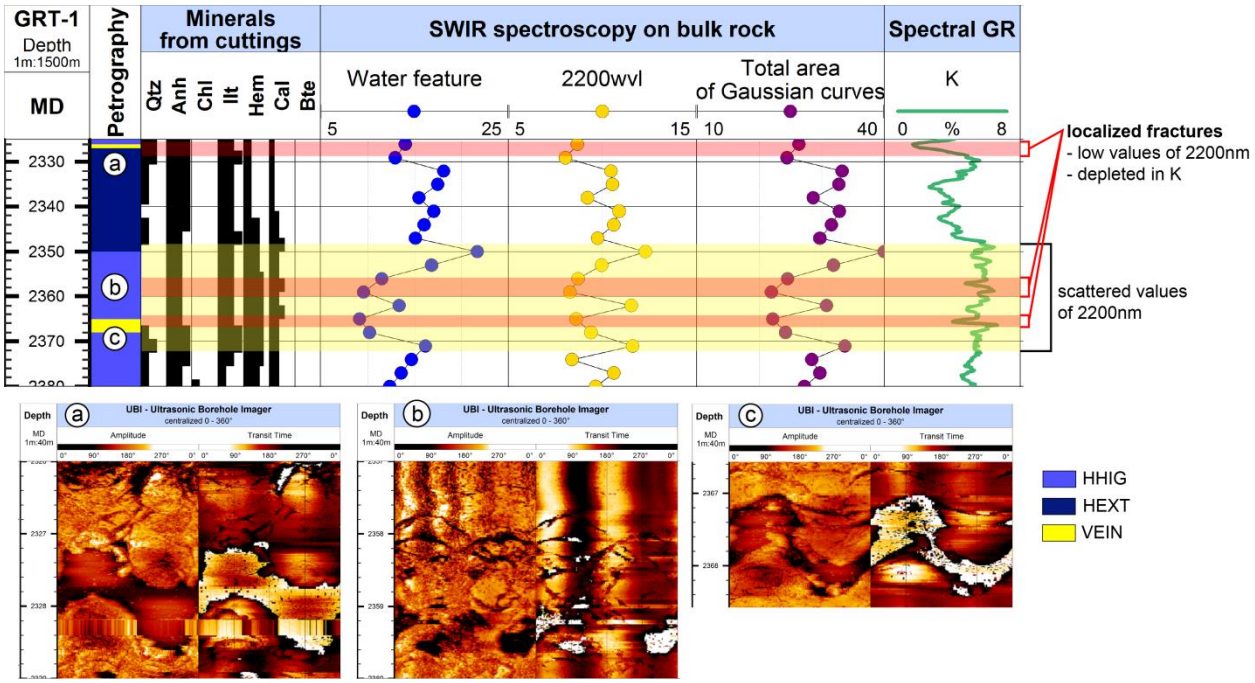


**Figure 6: Zoom on the main permeable FZ of the GRT-1 well, showing the petrography, the SWIR results with the water feature, 2200wvl and the total area, and the potassium (K). a. acoustic image log of the open fracture at 2328 m. b. acoustic image log of the open fracture at 2359 m c. acoustic image log of the open fracture at 2328 m.**

### 3.2. GPK-4 well

In the granitic part of the GPK-4 well, five sections are distinguished (Figure 7).

The deepest section, from 5260 to 4740 m MD (4990 to 4475 m TVD), is characterized by scattered values; the total area varies between 5 and 42 a.u., the water feature varies between 2 and 33 a.u. with an important increase from 4742 to 4900 m MD and the 2200wvl varies between 1 and 10 a.u.. This section corresponds to unaltered granite and two micas granite (GRAN, GR2M), with zones abundant in biotite.

The second section, from 4740 to 4000 m MD (4475 to 3823 m TVD) is characterized by stable and low values; around 8 a.u. for the total area, 4 a.u. for the water feature and 1 a.u. for the 2200wvl. This section corresponds to unaltered granite (GRAN).

The third section, from 4000 to 3600 m MD (3823 to 3475 m TVD) presents scattered values; from 8 to 25 a.u. for the total area, from 2 to 14 a.u. for the water feature and from 0.5 to 9 a.u. for the 2200wvl. This section corresponds to unaltered to low altered granite (GRAN, HLOW).

The fourth section from 3600 to 3200 m MD (3475 to 3128 m TVD) presents low and moderately scattered values; from 10 to 25 a.u. for the total area, from 3 to 10 a.u. for the water feature and from 1 to 4. a.u. for the 2200wvl. This section corresponds to unaltered to low altered granite (GRAN, HLOW).

Between the fourth and fifth section at 3200 m MD, a sharp change in the values of 2200wvl is observed. This is surely due to the change of facies, from unaltered granite to a section of altered granite. This phenomenon could be accentuated by the occurrence of drilling tool change at this same depth (Figure 7). A new drilling tool decreases the cutting size and thus the intensity of the SWIR signal is also lowest.

The fifth section from 3200 to 1400 m MD (3128 to 1400 m TVD) presents highly scattered values; from 15 to 60 a.u. for the total area, from 8 to 37 a.u. for the water feature, and from 1 to 19 for the 2200wvl. This section crosses grades of hydrothermal alteration, from low to high altered granite (HLOW, HMOD, HHIG). This section is associated to several temperature anomalies (Figure 7). More precisely from 1801 to 1813 m MD correlating to an increase of the 2200wvl, a cluster of opened and sealed fractures is observed with a main fracture at 1801 m MD associated to a temperature anomaly and mud losses (Dezayes et al., 2005).

The variability shows very stable and low values in comparison with the GRT-1 well. The highest variabilities are observed for the samples at

2235 m MD corresponding to a fracture observed on the acoustic image logs in the shallowest section between 1400 and 3200 m MD (Figure 8a).

Below this fracture at 2235 m MD, high and scattered values in the SWIR results are observed; from 23 to 55 a.u. in the total area, from 13 to 28 a.u. in the water feature and from 5 to 17 a.u. in the 2200wvl from 2235 to 2300 m MD (Figure 8). These high values correlate a FZ of open and sealed fractures observed on acoustic image log with halos of alteration from 2270 to 2273 m MD with the main fracture at 2270 m MD striking N-S and dipping eastward (Figure 8a and b). This FZ is associated to a thermal anomaly and permeability indicators.

At the top of the deepest large-scale cluster from 5260 to 4700m MD, another FZ correlates high peaks in the SWIR results (Figure 9). From 4700 to 4900 m MD the total area is from 8 to 43 a.u. and the water feature from 3 to 33 a.u. but very low and stable values around 1 a.u.for the 2200 wvl (Figure 9). The origin of high values for the water feature still has to be determined. Except at 4725 m where the 2200wvl is slightly higher (from 0 to 3 a.u.). At this depth, acoustic image log present partly opened fractures at 4722.5, 4724.5 and 4726 m MD. These fracture zones are associated with total mud losses observed during drilling operations as well as CH4 occurrences. But no thermal anomaly was measured.

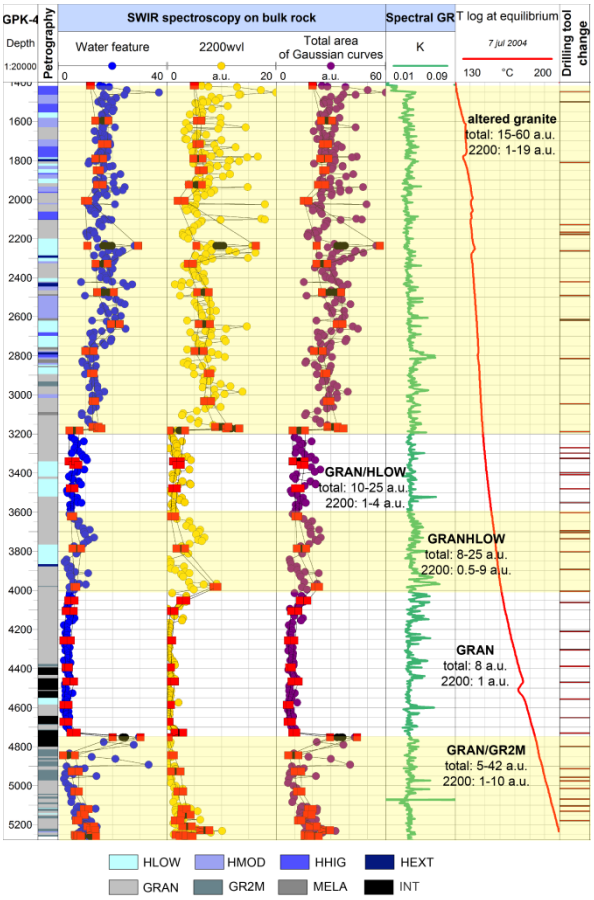


**Figure 7: Composite log of the GPK-4 well presenting the petrography observed on cuttings with the associated minerals quantity, the SWIR results with the water feature, 2200wvl and the total area, the potassium (K) from the spectral gamma ray (GR), the temperature log acquired at temperature equilibrium and the drilling tool change, (GR2M: two mica granite, MELA: biotite rich granite, INT: granite artificially enriched in biotite due to drilling process).**

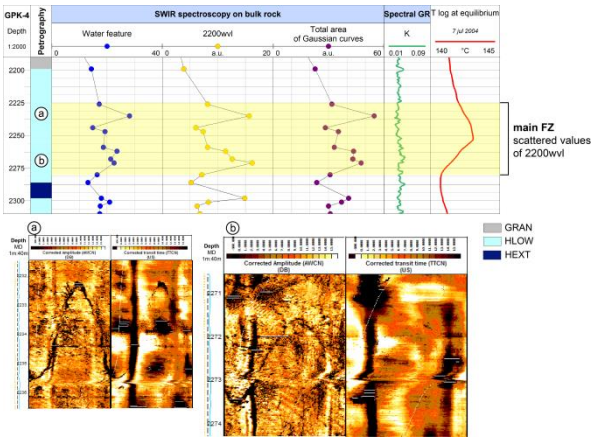


**Figure 8: Zoom on a FZ of the GPK-4 well, showing the petrography, the SWIR results with the water feature, 2200wvl and the total area, the potassium (K), and the temperature log. a. acoustic**

**image log of the fracture at 2234 m MD. b. acoustic image log of the fracture at 2273 m MD.**

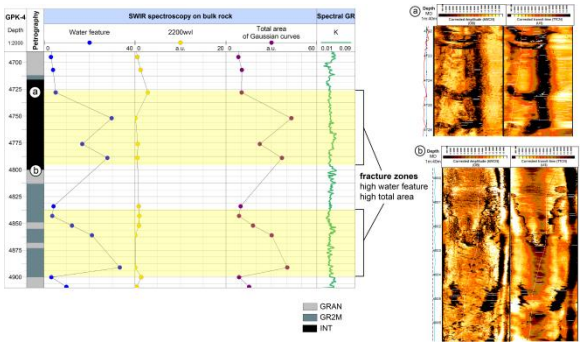


**Figure 9: Zoom on a FZ of the GPK-4 well, showing the petrography, the SWIR results with the water feature, 2200wvl and the total area, the potassium (K), and the temperature log. a. acoustic image log of the fracture at 4780 m MD. b. acoustic image log of the fracture at 4802 m MD.**

## 4. DISCUSSION

### 4.1. SWIR signal and alteration grades

In the unaltered granite, the SWIR signal is homogenous, stable and low, showing thus a good reproducibility of the measurements. Moreover, different responses of the SWIR signal are observed for the several hydrothermal alteration grades (Figure 10). In such sections, the scattering of the SWIR signal could mimics the heterogeneity of the altered facies. Hence a highly altered facies containing illite and small scale fractures filled by quartz will have a scattered 2200wvl response, alternating from low values (quartz veins) to very high values (illite) in opposition with the unaltered homogeneous granite (primary biotite partly chloritized). Higher the intensity of the 2200wvl is, higher the illite quantity is.

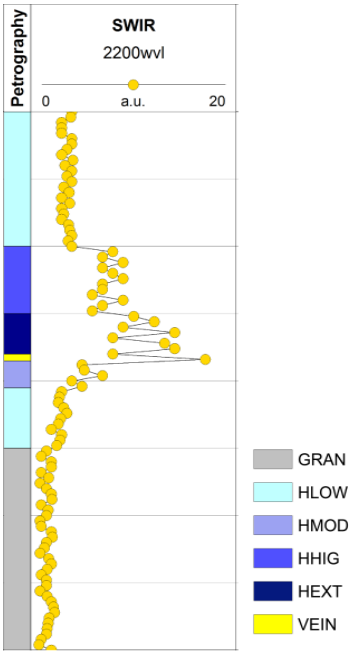


**Figure 10: Model of variation of the area of the 2200wvl in response to the different grades of hydrothermal alteration of the granite and to FZ.**

### 4.2. SWIR signal in FZs

The highest values of the 2200wvl are most of the time associated with damage zones related to open fractures visible on the acoustic image logs as well as permeable indicators (mud losses, temperature anomaly). At the same time, lowest values of the 2200wvl are associated with fracture cores which are materialized by quartz veins. As a result, FZs (core zone and damage zones) are characterized by great variability in 2200wvl values because of the high heterogeneity of cuttings a this depth (Figure 10).

It is also observed that the highest values of intra-sample variability are associated with FZs.

Illitization is thus in this geothermal system associated to present or fossil hydrothermal circulations.

### 4.3. Geothermal reservoirs

The GRT-1 well encounters the naturally permeable reservoir from the top of the granitic basement 2250 m MD to 2380 m MD (2236-2365 m TVD) which is characterized by high and scattered SWIR values (Figure 5). This section corresponds to a highly altered and fractured damage zone surrounding the main permeable fracture at 2368 m MD associated to a thermal anomaly (Figure 6).

The GPK-4 well encounters three permeable reservoirs:

- From the top of the granitic basement 1400 m MD to 3200 m MD (1400-3128 m TVD) a first shallow naturally permeable reservoir characterized by high and scattered SWIR values.

Localized very high anomalies of the 2200wvl correlate with permeable FZ as well as temperature anomalies.

- From 3200 to 4700 m MD (3128-4436 m TVD), a lowly permeable reservoir is characterized by very low and stable values corresponding to the unaltered granite (Figure 7). Inside this section, from 3600 to 4000 m MD, high values of the 2200wvl correlated with high GR values could correspond to paleo-altered FZ. Hence, there are no thermal anomalies associated because they are sealed by illite. Whereas at 4510 m MD, a thermal anomaly indicates a permeable FZ which is not visible on the SWIR signal at 2200wvl probably because of granite artificially enriched in biotite due to drilling process, INT facies (Dezayes et al., 2005).
- From 4700 to 5276 m MD (4436-5000 m TVD), a third lowly permeable reservoir is encountered. It is characterized by low but increasing SWIR values with depth (Figure 7). These values are surely due to the alternation between the two-mica granite (GR2M) and the porphyritic unaltered granite (GRAN) illustrating petrographic facies variations. However some sparse peaks of the 2200wvl are locally observed which could reflect the occurrence of individual partly opened fractures not visible on the temperature log. This lower values of the 2200wvl compared to the shallower reservoir could characterize lower productivity index (Schill et al., 2017). In the deepest granitic section, lower illite alteration could evidence less permeable fractures. It could be interpreted by a lower water-rock ratio and then a lower connection between the FZs and the reservoir. In parallel, in this deep zone, the present-day stress field could tend to close the natural fractures and then reduce the permeability. Moreover, in this deep zone, SWIR signal is higher and thus more impacted by the occurrence of petrographic variations.

From these interpretations, both GRT-1 and GPK-4 wells intersect the top of the most permeable granitic basement. At Soultz it is encountered from 1400 to 3128 m TVD and at Rittershoffen it is encountered from 2236 to 2365 m TVD (Figure 5 and 7). This section extending rhoughly on 1 km in-depth is characterized by a high density of fractures in all the Soultz wells (Dezayes et al., 2010; Dezayes and Lerouge, 2019; Genter et al., 1997b, 1997a; Valley, 2007). At Rittershoffen, in both geothermal wells, the very high values of the 2200wvl are also associated to highly permeable fractures (Vidal et al., 2018a). At Soultz, the analysis of SWIR data in other wells GPK-1, -2 and -3 is ongoing.

## 4. CONCLUSION

In this study, SWIR method has been applied to the Rittershoffen and Soultz geothermal wells. The method showed a good correlation between the SWIR signal and the hydrothermal alteration grades.

The SWIR at 2200wvl area reflects the occurrence of illite related to FZ. We assume that the intensity of this 2200wvl is an efficient proxy to the quantity of illite.

The SWIR method enables to characterize the signature of FZ by distinguishing the nature, extent and intensity of the hydrothermal alteration around permeable and non-permeable FZs.

## REFERENCES

Baujard, C., Genter, A., Dalmais, E., Maurer, V., Hehn, R., Rosillette, R., Vidal, J., Schmittbuhl, J., 2017. Hydrothermal characterization of wells GRT-1 and GRT-2 in Rittershoffen, France: Implications on the understanding of natural flow systems in the Rhine Graben. 65, 255–268pp. https://doi.org/10.1016/j.geothermics.2016.11.001

Dezayes, C., Chèvremont, P., Tourlière, B., Homeier, G., Genter, A., 2005. Geological study of the GPK4 HFR borehole and correlation with the GPK3 borehole (Soultz-sous-Forêts, France) (No. RP-53697-FR). BRGM, Orléans, France.

Dezayes, C., Genter, A., Valley, B., 2010. Structure of the low permeable naturally fractured geothermal reservoir at Soultz. C. R. Geoscience 342, 517–530. https://doi.org/10.1016/j.crte.2009.10.002

Dezayes, C., Lerouge, C., 2019. Reconstructing Paleofluid Circulation at the Hercynian Basement/Mesozoic Sedimentary Cover Interface in the Upper Rhine Graben. Geofluids 2019, 1–30. https://doi.org/10.1155/2019/4849860

Garnish, J.D., 1985. Hot Dry Rock - A European perspective. GRC Hawaï.

Genter, A., 1989. Géothermie roches chaudes sèches : le granite de Soultz-sous-Forêts (Bas-Rhin, France). Fracturation naturelle, altérations hydrothermales et interaction eau-roche. (PhD). Université d'Orléans, France.

Genter, A., Castaing, C., Dezayes, C., Tenzer, H., Traineau, H., Villemin, T., 1997a. Comparative analysis of direct (core) and indirect (borehole imaging tolls) collection of fracture data in the Hot Dry Rock Soultz reservoir (France). 102, 15,419-15,431.

Genter, A., Evans, K., Cuenot, N., Fritsch, D., Sanjuan, B., 2010. Contribution of the exploration of deep crystalline fractured reservoir of Soultz to the knowledge of enhanced geothermal systems (EGS). Comptes Rendus Geoscience 342, 502–516. https://doi.org/10.1016/j.crte.2010.01.006

Genter, A., Homeier, G., Chèvremont, P., Tenzer, H., 1999. Deepening of GPK-2 HDR borehole, 3880-5090m (Soultz-sous-Forêts, France). Geological Monitoring (No. R 40685). BRGM.

Genter, A., Traineau, H., 1996. Analysis of macroscopic fractures in granite in the HDR geothermal well EPS-l, Soultz-sous-Forets, France. Journal of Volcanology and Geothermal Research 121–141.

Genter, A., Traineau, H., Artignan, D., 1997b. Synthesis of geological and geophysical data at Soultz-sous-Forêts (France) (No. 39440). BRGM, Orléans, France.

Gérard, A., Kappelmeyer, O., 1987. The Soultz-sous-Forêts project. Geothermics 16, 393–399.

Gérard, A., Menjoz, A., Schwoerer, P., 1984. L'anomalie thermique de Soultz-sous-Forêts. Géothermie Actualités 35–42.

Glaas, C., Genter, A., Girard, J.F., Patrier, P., Vidal, J., 2018. How do the geological and geophysical signatures of permeable fractures in granitic basement evolve after long periods of natural circulation? Insights from the Rittershoffen geothermal wells (France). Geothermal Energy 6. https://doi.org/10.1186/s40517-018-0100-9

Hébert, B., 2018. Approche quantitative par spectrométrie Vis-NIR des minéraux argileux et uranifères dans les sables du gisement de Tortkuduk, Kazakhstan. Université de Poitiers, Poitiers.

Hooijkaas, G.R., Genter, A., Dezayes, C., 2006. Deep-seated geology of the granite intrusions at the Soultz EGS site based on data from 5km-deep boreholes. Geothermics, The deep EGS (Enhanced Geothermal System) project at Soultz-sous-Forêts, Alsace, France 35, 484–506. https://doi.org/10.1016/j.geothermics.2006.03.003

Kappelmeyer, O., 1991. European HDR project at Soultz-sous-Forêts general presentation. Geotherm. Sci. & Tech. 263–289.

Ledésert, B., Berger, G., Meunier, A., Genter, A., Bouchet, A., 1999. Diagenetic-type reactions related to hydrothermal alteration in the Soultz-sous-Forets Granite, France. European Journal of Mineralogy 11, 731–741.

Ledésert, B., Dubois, J., Genter, A., Meunier, A., 1993. Fractal analysis of fractures applied to Soultz-sous-Forets hot dry rock geothermal program. Journal of Volcanology and Geothermal Research 57, 1–17. https://doi.org/10.1016/0377-0273(93)90028-P

Ledésert, B., Hebert, R., Genter, A., Bartier, D., Clauer, N., Grall, C., 2010. Fractures, hydrothermal alterations and permeability in the Soultz Enhanced Geothermal System. Comptes Rendus Geoscience 342, 607–615. https://doi.org/10.1016/j.crte.2009.09.011

Ledésert, B., Hébert, R.L., Grall, C., Genter, A., Dezayes, C., Bartier, D., Gérard, A., 2009. Calcimetry as a useful tool for a better knowledge of flow pathways in the Soultz-sous-Forêts Enhanced Geothermal System. Journal of Volcanology and Geothermal Research 181, 106–114. https://doi.org/10.1016/j.jvolgeores.2009.01.001

Meller, C., Ledésert, B., 2017. Is There a Link Between Mineralogy, Petrophysics, and the Hydraulic and Seismic Behaviors of the Soultz-sous-Forêts Granite During Stimulation? A Review and Reinterpretation of Petro-Hydromechanical Data Toward a Better Understanding of Induced Seismicity and Fluid Flow. Journal of Geophysical Research: Solid Earth 122, 9755–9774. https://doi.org/10.1002/2017JB014648

Pontual, S., Merry, N., Gamson, P., 1997. G-Mex Vol.1, Spectral interpretation field manual. Ausspec international Pty. Ltd., Kew, Victoria 3101, Australia.

Rotstein, Y., Edel, J.-B., Gabriel, G., Boulanger, D., Schaming, M., Munschy, M., 2006. Insight into the structure of the Upper Rhine Graben and its basement from a new compilation of Bouguer Gravity. Tectonophysics 425, 55–70. https://doi.org/10.1016/j.tecto.2006.07.002

Sausse, J., Dezayes, C., Dorbath, L., Genter, A., Place, J., 2010. 3D model of fracture zones at Soultz-sous-Forêts based on geological data, image logs, induced microseismicity and vertical seismic profiles. Comptes Rendus Geoscience, Vers l'exploitation des ressources géothermiques profondes des systèmes hydrothermaux convectifs en milieux naturellement fracturés 342, 531–545. https://doi.org/10.1016/j.crte.2010.01.011

Sausse, J., Genter, A., 2005. Types of permeable fractures in granite. Geological Society, London, Special Publications 240, 1–14. https://doi.org/10.1144/GSL.SP.2005.240.01.01

Schill, E., Genter, A., Cuenot, N., Kohl, T., 2017. Hydraulic performance history at the Soultz EGS reservoirs from stimulation and long-term circulation tests 70, 110–124. https://doi.org/10.1016/j.geothermics.2017.06.003

Toby, B.H., 2006. R factors in Rietveld analysis: How good is good enough? Powder Diffraction 21, 67–70. https://doi.org/10.1154/1.2179804

Traineau, H., Genter, A., Cautru, J.-P., Fabriol, H., Chèvremont, P., 1992. Petrography of the granite massif from drill cutting analysis and well log interpretation in the geothermal

HDR borehole GPK-1 (Soultz, Alsace, France), in: Geothermal Energy in Europe - The Soultz Hot Dry Rock Project. Bresee, James C., Montreux, Switzerland, pp. 1–29.

Valley, B., 2007. The relation between natural fracturing and stress heterogeneities in deep-seated crystalline rocks at Soultz-sous-Forêts (France). (PhD). Université de Neuchâtel, Switzerland.

Vidal, J., Genter, A., 2018. Overview of naturally permeable fractured reservoirs in the central and southern Upper Rhine Graben: Insights from geothermal wells. Geothermics 74, 57–73. https://doi.org/10.1016/j.geothermics.2018.02.003

Vidal, J., Genter, A., Chopin, F., 2017. Permeable fracture zones in the hard rocks of the geothermal reservoir at Rittershoffen, France. Journal of Geophysical Research: Solid Earth 122, 4864–4887. https://doi.org/10.1002/2017JB014331

Vidal, J., Glaas, C., Hébert, B., Patrier, P., Beaufort, D., 2018a. Use of SWIR spectroscopy for the exploration of permeable fracture zones in geothermal wells at Rittershoffen (Alsace, France). Presented at the Geothermal Resources Council, Reno, USA, p. 10.

Vidal, J., Patrier, P., Genter, A., Beaufort, D., Dezayes, C., Glaas, C., Lerouge, C., Sanjuan, B., 2018b. Clay minerals related to the circulation of geothermal fluids in boreholes at Rittershoffen (Alsace, France). Journal of Volcanology and Geothermal Research 349, 192–204. https://doi.org/10.1016/j.jvolgeores.2017.10.019

Villemin, T., Bergerat, F., 1987. L'évolution structurale du fossé rhénan au cours du Cénozoïque : un bilan de la déformation et des effets thermiques de l'extension. Bull. Soc. géol. France 8, 245–255.

## ACKNOWLEDGEMENTS

The authors warmly thank Benoît Hébert for allowing them to use his in-house Visual Basic software (TSS), and also the Poitiers team for the use of the TerraSpec on the Soultz site. They warmly thank Chrystel Dezayes from BRGM for the host and the access to the Soultz cutting samples. The authors also acknowledge the EGS Alsace project funded by ADEME (French Agency for Environment), as well as GEIE EMC and ECOGI for providing the samples.